Imaging of enzyme replacement therapy using PET

Christopher P. Phenix[a,b,2], Brian P. Rempel[b,3], Karen Colobong[c], Doris J. Doudet[d], Michael J. Adam[a], Lorne A. Clarke[c], and Stephen G. Withers[b,1]

[a]Tri-University Meson Facility (TRIUMF), 4004 Wesbrook Mall, Vancouver, BC, Canada V6T 2A3; [b]Departments of Chemistry and Biochemistry, University of British Columbia, Vancouver, BC, Canada V6T 1Z1; [c]Child and Family Research Institute, Department of Medical Genetics, University of British Columbia, 950 W28th Avenue, Vancouver, BC, Canada V5Z 4H4; and [d]Department of Medicine, Division of Neurology, 2221 Wesbrook Mall, Vancouver, BC, Canada V6T 2B5

Edited* by Joanna S. Fowler, Brookhaven National Laboratory, Upton, NY, and approved April 29, 2010 (received for review March 14, 2010)

Direct enzyme replacement therapy (ERT) has been introduced as a means to treat a number of rare, complex genetic conditions associated with lysosomal dysfunction. Gaucher disease was the first for which this therapy was applied and remains the prototypical example. Although ERT using recombinant lysosomal enzymes has been shown to be effective in altering the clinical course of Gaucher disease, Fabry disease, Hurler syndrome, Hunter syndrome, Maroteaux-Lamy syndrome, and Pompe disease, the recalcitrance of certain disease manifestations underscores important unanswered questions related to dosing regimes, tissue half-life of the recombinant enzyme and the ability of intravenously administered enzyme to reach critical sites of known disease pathology. We have developed an innovative method for tagging acid β-glucocerebrosidase (GCase), the recombinant enzyme formulated in Cerezyme® used to treat Gaucher disease, using an ^{18}F-labeled substrate analogue that becomes trapped within the active site of the enzyme. Using micro-PET we show that the tissue distribution of injected enzyme can be imaged in a murine model and that the PET data correlate with tissue ^{18}F counts. Further we show that PET imaging readily monitors pharmacokinetic changes effected by receptor blocking. The ability to ^{18}F-label GCase to monitor the enzyme distribution and tissue half-life in vivo by PET provides a powerful research tool with an immediate clinical application to Gaucher disease and a clear path for application to other ERTs.

mechanism-based enzyme inhibition | PET Imaging | Lysosomal Storage diseases | Gaucher disease

The use of enzyme replacement therapies (ERT) to treat lysosomal storage diseases is increasing steadily as more recombinant enzymes become available. Central to the development of ERT for lysosomal storage disorders was the elucidation of carbohydrate-dependent receptor-mediated plasma membrane uptake and endosomal targeting of lysosomal enzymes. Consequently the enzymes employed must be administered in the appropriate glycoform. Although ERT has been demonstrated to be safe and efficacious in a number of lysosomal storage diseases (1), there are many unanswered questions related to appropriate dosing regimens; the ability of recombinant proteins to target key tissues, the in vivo half-lives of recombinant proteins in specific tissues as well as long term efficacy. Advancements in these key areas would significantly improve the design of recombinant proteins for clinical use and ensure the best clinical outcomes for treated patients. Many of these questions could be addressed by PET imaging. Here, we demonstrate a unique method for labeling a specific recombinant enzyme without modification of the exterior of the protein and highlight the potential of PET imaging for monitoring the biodistribution of therapeutic enzymes.

The satisfactory incorporation of ^{18}F onto biomolecules such as proteins, peptides, and antibodies is often very challenging as structural modifications introduced by the surface attachment of a radiolabel may alter the biological activity and/or physical and metabolic stability of the final conjugate. The ideal situation would involve the incorporation of a small radiolabel into the interior of the protein without significant perturbation of protein structure or of the behavior of the protein in vivo. Unfortunately the short half-life of ^{18}F (109.8 min) renders the incorporation of such labels during protein synthesis impossible. However, specific integration of an ^{18}F-label directly into the active site of an enzyme would avoid these issues, allowing imaging to be performed. Given the difficulties associated with labeling the interior of the protein, it is perhaps not surprising that no such studies have been reported for monitoring administered enzyme therapeutics.

Gaucher Disease was the first lysosomal storage disease to be treated by ERT and serves as the prototypical model for this therapeutic approach. Gaucher Disease results from a deficiency in GCase, a lysosomal β-glucosidase that catalyzes the hydrolysis of β-glucosylceramide (GlcCer) to ceramide and β-D-glucose. This enzyme plays a critical role in glycosphingolipid metabolism by its influence on ceramide homeostasis (see Fig. 1*A*). Mutations in the GCase gene (2) result in enzyme deficiency, which leads to primary accumulation of GlcCer and, through complex and poorly understood mechanisms, produces the symptoms of Gaucher Disease (3). Features common to all forms and thought to be mediated by GlcCer storage within tissue macrophages include hepatosplenomegaly, thrombocytopenia, and anemia.

Produced from Chinese hamster ovary cells, the first commercially available ERT, Cerezyme®, is a recombinant GCase modified to ensure that N-linked glycans contain terminal mannose residues, thereby conferring high affinity for the mannose receptor resident on macrophages and other cell types (4) (See Fig. 2). GCase belongs to a class of β-glycosidases that catalyze the hydrolysis of glycosidic bonds via a two step, double displacement mechanism utilizing a pair of glutamic acid residues (see Fig. 1*B*) (5). In GCase, Glu340 acts as the catalytic nucleophile, displacing the ceramide moiety from the anomeric carbon of glucose to form a covalent glucosyl-enzyme intermediate (6). When presented with substrate analogues in which the 2-hydroxyl has been replaced by fluorine and a reactive leaving group installed at the anomeric carbon (C-1), such enzymes form a long-lived covalent glycosyl-enzyme intermediate (7) (see Fig. 1*B*). Importantly, structures of several such trapped intermediates reveal that no significant protein conformational changes accompany formation of this intermediate, thus its biodistribution is not expected to differ from that of free enzyme (8). If synthesized with a radioactive ^{18}F in place of the stable and common ^{19}F isotope, these inhibitors could serve as covalent, active-site directed, radioactive labeling agents of GCase. Once radioactively labeled with the

Author contributions: C.P.P., B.P.R., D.J.D., M.J.A., L.A.C., and S.G.W. designed research; C.P.P., B.P.R., and K.C. performed research; M.J.A. contributed new reagents/analytic tools; C.P.P., D.J.D., L.A.C., and S.G.W. analyzed data; and C.P.P., D.J.D., L.A.C., and S.G.W. wrote the paper.

The authors declare no conflict of interest.

*This Direct Submission article had a prearranged editor.

[1]To whom correspondence should be addressed. E-mail: withers@chem.ubc.ca.

[2]Present address: Thunder Bay Regional Research Institute, 290 Munro Street, Thunder Bay, ON, Canada P7A 7T1.

[3]Present address: Department of Science, The University of Alberta, Augustana Campus, 4901–46 Avenue, Camrose, AB, Canada T4V 2R3.

This article contains supporting information online at www.pnas.org/lookup/suppl/doi:10.1073/pnas.1003247107/-/DCSupplemental.

www.pnas.org/cgi/doi/10.1073/pnas.1003247107

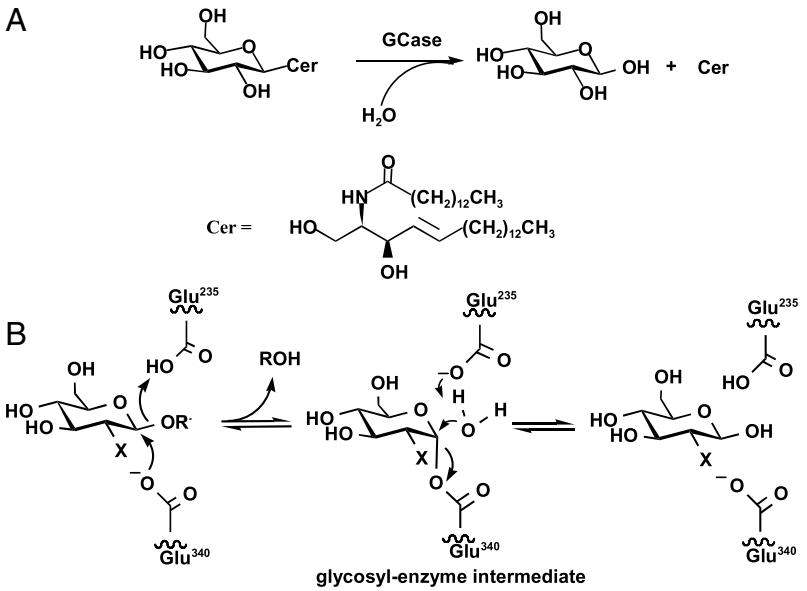

Fig. 1. The biochemical reaction catalyzed by GCase and the mechanism of catalysis *A*) Reaction catalyzed by GCase during glycosphingolipid metabolism *B*) Double displacement mechanism used by GCase when X = OH and OR = ceramide. When the 2-OH is replaced by F and the Ceramide replaced by 2, 4-dinitrophenol, these substrate analogues form a long-lived covalent glycosyl-enzyme intermediate.

positron-emitting ^{18}F isotope, noninvasive biodistribution studies of the therapeutic enzyme are possible using PET.

Results and Discussion

Radiochemical Labeling of β-Glucosidases. The development of a suitable ^{18}F-labeled mechanism-based inhibitor for β-glucosidases required the exploration of several different means of incorporating the isotopic label. While an attractive choice was to incorporate ^{18}F at the C-2 position, an alternative option was to presynthesize the cold 2-fluoro sugar fluoride and incorporate the ^{18}F isotope at a remote position on the sugar structure. In our initial attempts we radiochemically synthesized and tested two activated [^{18}F]-fluoroglycoside derivatives: 2-deoxy-2-fluoro-β-mannosyl fluoride, and 2, 6-dideoxy-2, 6-difluoro-β-glucosyl fluoride (9, 10). The former could be readily synthesized by $^{18}F_2$ addition to a protected D-glucal, while the latter could be generated by $^{18}F^-$ displacement of a 6-sulfonate derivative of 2-deoxy-2-fluoro-β-glucosyl fluoride. However, each agent suffered from either a lengthy synthesis or low bioconjugation rates, thus neither were useful.

Based upon published kinetic data for inactivation of GCase, we hypothesized that the ideal radiolabeled reagent might be 2-deoxy-2-[^{18}F]-fluoro-β-D-glucosyl fluoride, which is known to react reasonably rapidly with GCase ($k_i/K_i = 20\ M^{-1}\ min^{-1}$) (6). Unfortunately, synthesis of this compound would involve three chemical steps after ^{18}F incorporation, making its assembly too time-consuming. An alternative reagent would be 2, 4-dinitrophenyl 2-deoxy-[^{18}F]-2-fluoro-β-D-glucopyranoside (β-DNP-[^{18}F]-FDG) since the cold version of this compound is a known inactivator of other β-glucosidases, but was unknown as an inactivator of GCase (7). We therefore synthesized the cold version of this compound and confirmed it to be an inactivator with a comparable inactivation rate constant to that of 2-deoxy-2-fluoro-β-D-glucosyl fluoride for GCase ($k_i/K_i = 12\ M^{-1}\ min^{-1}$). This result opened up the attractive option of a one-step synthesis of β-DNP-[^{18}F]-FDG directly from pharmaceutical grade 2-deoxy-[^{18}F]-2-fluoro-D-glucose ([^{18}F]-FDG), the most widely used PET radiopharmaceutical. If we could optimize reported procedures (11) for the direct formation of dinitrophenyl glycosides from free sugars plus fluorodinitrobenzene, an ^{18}F glucosidase labeling agent amenable to PET imaging would be produced. Indeed, by iterative optimization of reaction conditions, varying base, concentration, temperature, and reaction time we developed a rapid, efficient, and stereoselective coupling process between FDG and fluoro-2, 4-dinitrobenzene that is achievable at most radiochemical facilities that synthesize [^{18}F]-FDG (see *Materials and*

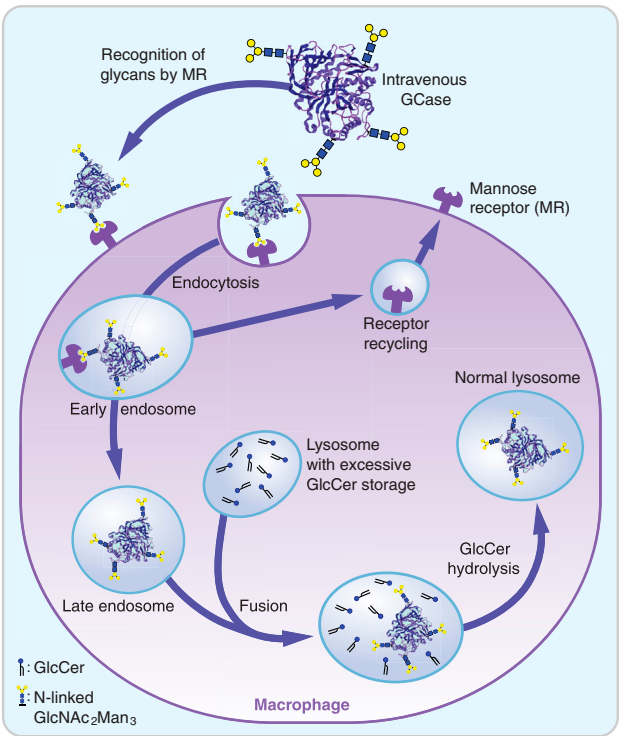

Fig. 2. Macrophage uptake of intravenously administered recombinant GCase (structure used in this figure taken from Dvir et al. (21)). The recombinant GCase in Cerezyme, produced from Chinese hamster ovary cells, is modified to ensure that N-linked glycans contain terminal mannose residues thus conferring high affinity for the mannose receptor (MR) resident on the macrophage and other cell types. Internalization of the enzyme occurs through endocytosis of the MR receptor/GCase complex. Early endosomes containing GCase mature into late endosomes while receptor sorting leads to the recycling of the MR receptor back to the cellular membrane. Late endosomal and lysosomal fusion delivers the therapeutic enzyme to the lysosome which subsequently restores GlcCer to normal levels.

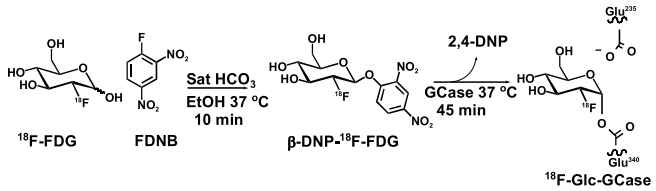

Fig. 3. Radiochemical synthesis of the glycosidase labeling agent β-DNP-[^{18}F]-FDG and active-site labeling of GCase.

Methods and Fig. 3). HPLC and radio-TLC (RTLC) analysis using authentic standards revealed that the major radioactive species present after 10 min reaction was the desired β-DNP-[^{18}F]-FDG (~80% radiochemical yield) with some [^{18}F]-FDG remaining and a third unidentified species that did not interfere with enzymatic labeling and was easily removed by gel filtration (see Fig. S1). Interestingly no 2, 4-dinitrophenyl 2-deoxy-[^{18}F]-2-fluoro-α-D-glucopyranoside was detected by HPLC. This finding is consistent with earlier studies of this arylation reaction, which revealed that the reaction was under kinetic control, with predominant formation of the β-glycoside being due to the greater reactivity of the β-hemiacetal in conjunction with rapid equilibration of the α- and β-hemiacetal anomers of the unreacted sugar. (12, 13) Indeed the reaction yield and selectivity were sensitive to temperature as no significant amounts of β-DNP-[^{18}F]-FDG were formed at shorter reaction times, neither at room temperature, nor at temperatures higher than 40 °C.

Radiolabeling of Abg and GCase. Two different enzyme systems were employed in the evaluation of approaches and reagents. Initial studies were performed on the well characterized β-glucosidase from *Agrobacterium* sp. (Abg). Abg is a stable, easily handled enzyme that has been extensively studied by our group (14, 15). Having worked out ideal conditions and proven the active-site location of the label, studies were then performed on the therapeutically relevant enzyme GCase.

Covalent inactivation of Abg by β-DNP-FDG is known to occur rapidly, with a second-order rate constant for formation of the covalent fluoroglucosylated-ABG (F-Glc-Abg) intermediate (k_i/K_i) of 500 mM^{-1} min^{-1}. As expected, incubation of freshly synthesized β-DNP-[^{18}F]-FDG with Abg resulted in the formation of radioactive enzyme within several minutes. By contrast, GCase is inactivated at a much lower rate (k_i/K_i of 0.012 mM^{-1} min^{-1}), largely due to a much higher K_i value, and consequently required longer incubation times for radioactive labeling. To minimize this problem, β-DNP-[^{18}F]-FDG recovered from the HPLC was evaporated to dryness and dissolved in minimal amounts of assay buffer (<200 μL) prior to addition of concentrated GCase to keep its concentration as high as possible. Reaction times required for the radioactive tagging of GCase were still significantly longer than for Abg, typically about 45 min in total, but now consistent with the requirements for isotopic labeling with ^{18}F required for PET imaging. As seen in the RTLC analysis shown in Fig. S2, efficient labeling was observed.

Demonstration That ^{18}F Labeling Occurs in the Enzyme's Active Site. While the ^{18}F tagging of both enzymes was demonstrated by RTLC and size exclusion chromatography, we required further evidence that the labeling chemistry was occurring in the active sites of each enzyme. A variety of control experiments on GCase and Abg, including protection against inactivation and acceptor-dependent reactivation, demonstrated that radioactive tagging was active-site-specific, as follows.

Mutant Abg lacking the catalytic nucleophile is not radioactively tagged. To demonstrate that the radioactive labeling of Abg was dependent on the intact catalytic machinery of the enzyme, we used a mutant Abg (Abg E358A) possessing an identical primary sequence to natural Abg, except that the active-site nucleophile, Glutamic acid 358, was mutated to an Alanine (16). Such enzymes have been shown to be catalytically incompetent, although they still retain their secondary and tertiary structure (17). RTLC analysis revealed that incubation of β-DNP-[^{18}F]-FDG with Abg E358A did not result in radioactive tagging of the protein, clearly demonstrating that the fully intact catalytic machinery in the active site of natural Abg is vital for the radioactive labeling of the enzyme, and ruling out the incorporation of ^{18}F in a nonspecific manner.

Reactivation of the ^{18}F-fluoroglycosylated form of Abg. The F-Glc-Abg intermediate is a stable but catalytically competent species that breaks down very slowly by hydrolysis ($t_{1/2}$ = 57,000 min) but undergoes more rapid reactivation by transglycosylation onto catalytically relevant sugars. Consistent with this, the addition of 20 mM thiophenyl β-D-glucopyranoside (TG) to the F-Glc-Abg intermediate accelerates the transglycosylation reaction ($t_{1/2}$ = 53 min) resulting in the formation of a new disaccharide and regeneration of the catalytically active Abg enzyme (see Fig. S3) (18). We employed this reactivating agent as an important control to demonstrate that the radiolabeling of Abg was in fact mediated through the 2-fluoroglucosyl-Abg intermediate in the active site of the enzyme. Treatment of ^{18}F-Glc-ABG with 60 mM TG resulted in the relatively rapid formation of a new radioactive peak possessing an R_f corresponding to a neutral phenyl glycoside, along with a proportional decrease in the peak for ^{18}F-Glc-ABG (see Fig. S4). The time scale of this reaction was consistent with the previously measured half-life, thereby providing solid evidence that the radioactive tagging of Abg is through a covalent ^{18}F-fluoroglycosyl-enzyme intermediate. Due to the known, very slow turnover of the 2-fluoroglucosyl enzyme intermediate on GCase ($t_{\frac{1}{2}}$ > 1,300 min) it was not possible to perform the equivalent controls on this enzyme with ^{18}F-labeled reagents ($t_{\frac{1}{2}}$ = 109.8 min) (6).

Inhibition of GCase labeling by 6-nonylisofagomine. In order to demonstrate that GCase labeling was an active-site-dependent process, radioactive tagging was attempted in the presence of 6-nonylisofagomine, a potential active-site-specific chaperone known to be a potent inhibitor (IC_{50} = 0.6 nM) of the enzyme (see Fig. S5) (19). Indeed, incubation of GCase with β-DNP-[^{18}F]-FDG and 6-nonylisofagomine under identical conditions to those used previously resulted in no incorporation of radiolabel into the enzyme.

Isolation of Radiochemically Pure ^{18}F-Glc-GCase. Performance of biodistribution studies of ^{18}F-Glc-GCase in mice, required access to radiochemically pure ^{18}F-Glc-GCase. Initial attempts to remove excess β-DNP-[^{18}F]-FDG and other radioactive molecules by HPLC using several different gel filtration columns failed as GCase was retained in the matrix of the gel, a behavior reported previously (20). Fortunately, it was found that GCase remains soluble at high concentrations in 50 mM MES buffer containing 150 mM NaCl without the need for stabilizing detergents (21). By sequential repetitive dilution of the taurocholate and Triton-X100 with MES buffer and concentration by ultrafiltration using Centricon 50 kDa centrifugal devices, the radiolabeled enzyme was concentrated, while simultaneously removing excess β-DNP-[^{18}F]-FDG and other contaminating small molecules. A final clean up step and buffer exchange was accomplished using a desalting spin column previously saturated with buffer. Following this procedure, we were able to routinely isolate about 200 μCi of radiochemically pure ^{18}F-Glc-GCase (see Fig. S6) for PET studies in about 2.5 h, including all radiochemical steps. This synthesis should be scalable to permit clinical imaging of Gaucher patients. However, to limit radiation exposure to the

radiochemist, automation of the chromatography steps would be required but is entirely feasible.

Biodistribution and PET Imaging of ^{18}F-Glc-GCase. To study the in vivo biodistribution of GCase, radiochemically pure ^{18}F-Glc-GCase was administered as a bolus tail vein injection into healthy mice, and the tissue distribution analyzed both by measuring the amounts of radioactivity in postmortem tissue samples and non-invasively using micro-PET. Radioactive uptake was observed in various tissues and organs (see Fig. 4*A*), and data compared favorably to the limited GCase biodistributions previously reported based on enzymatic assays of tissue homogenates (22–24). Macrophage-rich organs such as the liver and spleen demonstrated the highest overall uptake. Interestingly, uptake was also observed in the gall bladder, bones (femur, vertebrae, pelvis, and shoulders), bone marrow, kidneys, intestines, thymus, and transiently in the heart. Insignificant amounts of radioactivity were detected in the brain, and skeletal muscle. Blood sampling by heart puncture at the end of some studies revealed that, by 1 h postinjection, very little radioactivity remained in the circulation (<0.5% injected dose), thereby demonstrating rapid enzyme uptake by some tissues. Tissue activity in micro-PET studies correlated well with the data obtained from tissue activity counts from killed animals (see Fig. 4*B*) and images were reconstructed to illustrate organ uptake (see Fig. 5 *A* and *B*). Higher resolution analysis such as cellular distribution is precluded by the inherent spatial limitations of the PET technique. Elimination of ^{18}F-Glc-GCase was observed through renal and hepatobiliary routes as radioactivity was detected in the urinary bladder, gall bladder, and large intestine in later time points. Renal elimination is not surprising given that the molecular mass of the recombinant GCase is ~60 kDa (25), and the molecular weight cut off value for glomerular filtration is estimated to be about 60 kDa (26). Different biodistributions may be observed if the labeled enzyme is administered by infusion rather than as a bolus injection.

An advantage of using [^{18}F]-FDG as the radioactive tag is that, in the event of enzymatic turnover or proteolytic degradation of ^{18}F-Glc-GCase, the resulting radioactivity released as [^{18}F]-FDG would be rapidly phosphorylated by hexokinase and unlikely to enter back into circulation within the time frame of the scan. However, even this scenario is unlikely since ^{18}F-Glc-GCase has a half-life of hydrolysis of 1,300 min in vitro, with a similar rate being observed in mice (27). Significant release of [^{18}F]-FDG from the active site through spontaneous hydrolysis or metabolic breakdown of ^{18}F-Glc-GCase is therefore highly unlikely to compromise the biodistribution data over the 2 h micro-PET acquisition time.

Receptor Blocking Experiments. In order to test the ability of this imaging approach to readily and noninvasively monitor how the enzyme biodistribution can be controlled through coadministration of external agents, or possibly by modifying surface glycan structures on the enzyme, receptor blocking experiments were performed. The macrophage uptake of glycoproteins such as recombinant GCase from the circulatory system relies on surface glycans terminating in mannose and N-acetylglucosamine, and primarily occurs through the mannose/N-acetylglucosamine (MR) receptor system and other receptor types (28) (Fig. 2). The mannose receptor-ligand complex is rapidly internalized and recycling of new receptors is thought to occur (29). To demonstrate that radioactive uptake in the liver was mannose receptor-dependent and to determine the ability of the PET-imaging approach to monitor changes in uptake, we performed a receptor blocking experiment by the intravenous administration of mannan prior to injection of ^{18}F-Glc-GCase. As can be seen in Fig. 4 *C* and *D* and Fig. 5 *C* and *D*, a significant decrease in the rate of uptake by the liver was observed for mice pretreated with mannan when compared to control mice receiving only ^{18}F-Glc-GCase. After 2 h the total amounts of ^{18}F-Glc-GCase accumulating in the liver of the mannan-treated mice approached that of the control mice, consistent with decreasing tissue mannan concentrations and receptor recycling. These results demonstrate how this PET-imaging approach

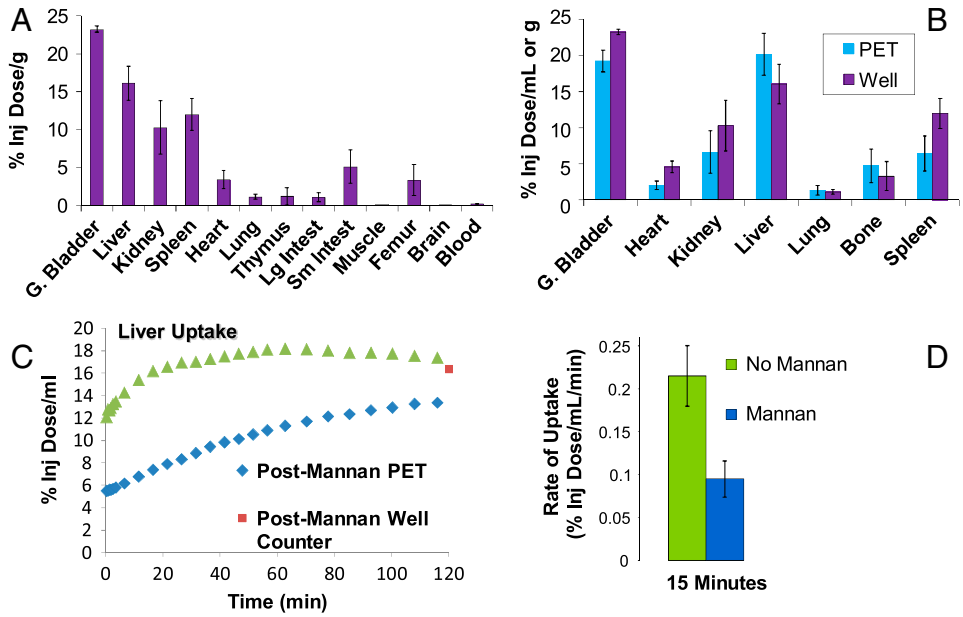

Fig. 4. Uptake of ^{18}F-Glc-GCase in various organs. *A*) Biodistribution of ^{18}F-Glc-GCase in various tissues at 2 h postinjection in mice. Mice were killed and tissue radioactivity was measured by γ counting ($n = 4$ for all organs except the gall bladder where $n = 2$) *Bars* represent the average tissue uptake plus/minus standard deviation (expressed as % injected dose/g of tissue). *B*) Comparison of the biodistribution of ^{18}F-Glc-GCase as determined by PET (*blue bars* expressed % injected dose/mL) and by postmortem tissue γ counting (*purple bars* expressed % injected dose/g) 2 h postinjection. *C*) Liver uptake of ^{18}F-Glc-GCase determined by PET in an untreated (*green triangles*) and a mannan-treated mouse (*blue diamonds*). The *red square* represents the postmortem tissue activity counts of the mannan-treated mouse 2.5 h postinjection *D*) *Bar graphs* comparing the rate of liver uptake for untreated mice vs mice receiving yeast mannan (15 mg/kg) prior to injection of ^{18}F-Glc-GCase ($n = 2$ in each instance). The rates of uptake were determined by calculating the slope of the linear portion of the liver uptake curves over the first 15 min postinjection.

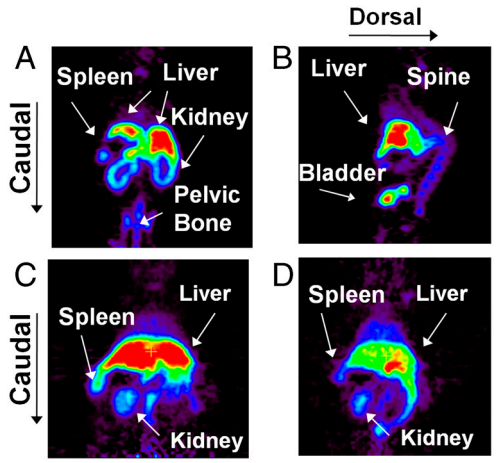

Fig. 5. PET images obtained by injection of ^{18}F-Glc-GCase into mice. Images are as follows: *A*) Coronal slice highlighting the accumulated uptake of tracer in spleen, kidneys, and liver over 2 h acquisition time *B*) Sagittal slice of the image shown in *A*) but highlighting the liver, bladder, and spine *C*) For comparison purposes the accumulated tracer uptake into organs of an untreated mouse summed over the first 20 min postinjection *D*) Accumulated tracer uptake into the organs of a mouse treated with mannan summed over the first 20 min postinjection

will allow direct analysis of the consequences of modification of administration protocols as well as administered reagents without bias arising from the modification of the exterior of the protein.

Conclusion

In summary, we have developed a unique mechanism-based method for radioactively labeling β-glycosidases using β-DNP-[^{18}F]-FDG derived from the widely available [^{18}F]-FDG, and used this method to monitor the biodistribution of the therapeutic enzyme GCase in mice. Our preliminary results indicate that PET-imaging may be useful in detailed studies of ERT including pharmacokinetic analysis of enzyme uptake in various tissues in vivo, as well as in the development of methods to alter tissue distribution and refine the targeting of recombinant proteins. This noninvasive technology could be applicable to Gaucher Disease patients and as such should provide valuable insights into the pharmacokinetic properties of recombinant enzyme and the role of personalized dosing regimens based on these in vivo studies. In addition, this PET-imaging approach will enable direct in vivo comparison of the recently introduced preparations of recombinant GCase derived from plant and human sources (30, 31). Currently, experiments are being designed to analyze the distribution of ^{18}F-Glc-GCase in mice with a conditional knock out of the GCase gene (32).

Materials and Methods

Radiosynthesis of DNP-[^{18}F]-FDG. Pharmaceutical grade 2-deoxy-2-[^{18}F]-fluoro-D-glucose (2-[^{18}F]-FDG) was a gift from the BC Cancer Agency, Vancouver Canada. The 2-[^{18}F]-FDG was synthesized using a commercially available automated radiochemistry system TRACER$_{lab}$ FX$_{FDG}$ following the manufacturer's instructions. Briefly, the system facilitates the automated synthesis of 2-[^{18}F]-FDG via nucleophilic displacement of the peracetylated mannose triflate with [^{18}F]-fluoride prepared by cyclotron bombardment of 1 mL of $H_2{}^{18}O$ with 12.5 MeV protons in a niobium target. Following deprotection with HCl a series of solid phase extraction (SPE) columns yield radiochemically pure 2-[^{18}F]-FDG in an isotonic solution (10% NaCl). After quality control analysis had ruled out the presence of [^{18}F]-fluoride, 10–15 mCi of 2-[^{18}F]-FDG was placed into a 2 mL v-vial containing a small stir bar and fitted with a rubber septum. The H_2O was evaporated by heating to 100 °C while simultaneously passing helium gas through the v-vial vented into a sodium lime trap. The vial was cooled to 37 °C after which 150 μL of aqueous $NaHCO_3$ (~0.93 M) and 150 μL of 1-fluoro 2, 4-dinitrobenzene in ethanol (~13 mg/mL) was added. The reaction was stirred for 10 min at 37 °C, quenched with acetic acid (25 μL) and evaporated at 60 °C as described above. The yellow residue was dissolved in 300 μL of distilled water, and loaded onto a C18 Sep Pak column (preequilibrated with 1 mL of H_2O) and a further 1 mL of H_2O was passed through the Sep Pak, collecting four fractions of approximately 0.33 mL. The second fraction containing the bulk of the radioactivity (generally between 3–5 mCi) was purified on a Synergy semiprep reverse phase HPLC column (Phenomenex) using a gradient of 60% CH_3OH/40% H_2O to 100% CH_3OH over 10 min. The solvent composition was maintained at 100% CH_3OH for a further 10 min. The DNP-[^{18}F]-FDG was collected in a 2.0 mL v-vial at approximately 14 min in mobile phase which consisted of a high percentage of CH_3OH, which was evaporated at 60 °C.

Kinetic Analysis of the Inactivation of GCase by β-DNP-FDG. β-DNP-FDG was chemically synthesized as described previously (7). To measure inactivation rates, varying concentrations of β-DNP-FDG in assay buffer (180 μL total volume, 20 mM citrate, 60 mM phosphate, pH 5.5, containing 1 mM EDTA, 0,25% (v/v) Triton X-100, and 0.25% taurocholate) were warmed to 37 °C. The inactivation was initiated by the addition of GCase (20 μL, 0.5 μg/mL) obtained from the unused portions of patient vials and diluted into assay buffer. At appropriate time points, 20 μL aliquots were withdrawn and added to a solution containing 2–10× the Michaelis constant, Km of 2, 4-dinitrophenyl β-D-glucopyranoside, along with a large volume of buffer (600 μL) warmed to 37 °C. This halts the inactivation reaction both by dilution of the β-DNP-FDG and by competition with a large excess of substrate. The residual enzyme activity was then assayed using a continuous enzymatic assay monitoring the rate of release of 2, 4-dinitrophenolate (2, 4-DNP) at a wavelength of 400 nm. The rate of 2, 4-DNP release is directly proportional to the concentration of catalytically active enzyme remaining in the solution. Pseudo-first order rate constants for the loss of enzymatic activity for each concentration of inactivator were determined by nonlinear fitting of the decay curve to a single exponential decay equation using GraFit. The individual k_{obs} values were then replotted as a function of inactivator concentration. Individual values for k_i and K_i were obtained by fitting to the equation:

$$k_{\text{obs}} = k_i[\text{I}]/K_i + [\text{I}].$$

Radiolabeling of Abg and Control Experiments. To a v-vial containing an evaporated DNP-[^{18}F]-FDG reaction mixture, Abg in phosphate buffer (50 mM, pH 6.5) was added and the solution incubated for 5 min at 37 °C. RTLC and size exclusion chromatography revealed the rapid formation of ^{18}F-Glc-Abg. To demonstrate that radioactive labeling was occurring in the active site of Abg, a mutant Abg (Abg E358A) was incubated with DNP-[^{18}F]-FDG as described for natural Abg. For the reactivation experiments, Abg was radiolabeled as described above followed by addition of thiophenyl glucoside (TG) to a final concentration of 60 mM. Samples were taken at various time points and analyzed by RTLC.

Radiolabeling and Isolation of GCase. To the v-vial containing the freshly purified DNP-[^{18}F]-FDG, recombinant GCase (~60 units obtained from the unused portions of patient vials of Cerezyme) in ~250 μL of reaction buffer (20 mM phosphate, 40 mM citrate, 0.25% sodium taurocholate, 0.1% Triton X-100, pH 5.5) was added and the solution incubated for 45 min at 37 °C. The solution was then diluted to a volume of ~1,000 μL by MES buffer (50 mM MES, 100 mM NaCl, pH 6.5) and divided between two Microcon centrifugal filter devices (50 kDa MW cut off), spun for 8 min at 14,000 x *g* in a Beckman centrifuge. Another portion of MES buffer (500 μL) was added and centrifuged for an additional 8 min. Final concentrate volumes were ~100 μL, which were then subjected to two rounds of gel filtration using Pierce Desalting Spin Columns following the manufacturer's instructions. Desalting columns were preequilibrated with Cerezyme buffer (60 mM Citrate, 20 mM Phosphate, 0.1% Tween 80 polysorbate^{80}, pH 6.6). Approximately 200 μCi of radiochemically pure (>97% by radio-TLC) ^{18}F-Glc-GCase possessing a specific activity of ~50 Ci/mmol was routinely synthesized following this method. Radioactive labeling of GCase can be blocked by the inclusion of 6-nonylisofagomine (10 mM) in the radiolabeling buffer mixture.

Micro-PET Imaging. Mice (C57BL/6 and 20 w of age $n = 4$) were subjected to inhalational isofluorane anesthesia (5% gas initial dose and then maintained at 1–2% gas with a mask). Once the animal was anesthetized, it was placed flat on its belly and taped to the scanner bed. Approximately 25–50 μCi of ^{18}F-Glc-GCase (~80 Units/kg) in approximately 50–100 μL of Cerezyme buffer was intravenously administered into the tail vein as a bolus injection. All studies were performed on a Siemens/Concorde Focus 120 micro-PET scanner. Following a 6 min transmission scan with a ^{57}Co source, a 2 h emission scan was performed starting at tracer injection. Data were histogrammed into 4 · 30, 2 · 60, 11 · 300, 6 · 450, and 2 · 480 s frames and reconstructed using Fourier rebinning and filtered backprojection after applying normalization,

scatter, attenuation, and sensitivity corrections. Two mice were similarly injected with the tracer but were used only for blood sampling and tissue counting and were killed at 1 hr postinjection. All the animals were euthanized prior to recovery from anesthesia by cervical dislocation and tissues were harvested for gamma counting within the PET unit. Regions of interest were chosen guided by the use of a mouse organ atlas. For the mannan blocking experiments, 15 mg/kg of mannan were injected into the tail vein 5–10 min prior to ^{18}F-Glc-GCase ($n = 2$ mice). All biodistribution data were decay corrected using a half-life of 109.8 min for the ^{18}F isotope. All procedures involving mice were approved by the University of British Columbia Animal Care Committee.

ACKNOWLEDGMENTS. We thank Siobhan McCormick and Katie Dinelle for performing the micro-PET scans and data acquisition, Harmony Hemmelgarn and Rajwinder Dhami for assistance with animal studies. We are grateful to Milan Vuckovic and Yulia Rozen of the BC Cancer agency for providing us with FDG for our synthesis. Many thanks to the people in the Nuclear Medicine division at TRIUMF for their technical assistance. A thank you also goes out to Dr. Ethan Goddard-Borger for covering due to illness and Dr. Tom Wennekes for producing Fig. 2. We acknowledge the financial support of the Canadian Institutes of Health Research, the Natural Sciences and Engineering Research Council of Canada, the Children's Gaucher Research Fund and the National Gaucher Foundation (US).

1. Rohrbach M, Clarke JTR (2007) Treatment of lysosomal storage disorders—progress with enzyme replacement therapy. *Drugs* 67:2697–2716.
2. Liou B, et al. (2006) Analyses of variant acid beta-glucosidases—effects of Gaucher Disease mutations. *J Biol Chem* 281:4242–4253.
3. Fuller M, et al. (2008) Glucosylceramide accumulation is not confined to the lysosome in fibroblasts from patients with Gaucher Disease. *Mol Genet Metab* 93:437–443.
4. Sato Y, Beutler E (1993) Binding, internalization, and degradation of mannose-terminated glucocerebrosidase by macrophages. *J Clin Invest* 91:1909–1917.
5. Kempton JB, Withers SG (1992) Mechanism of Agrobacterium beta-glucosidase—kinetic studies. *Biochemistry* 31:9961–9969.
6. Miao SC, et al. (1994) Identification of Glu(340) as the active-site nucleophile in human glucocerebrosidase by use of electrospray tandem mass-spectrometry. *J Biol Chem* 269:10975–10978.
7. Withers SG, Street IP, Bird P, Dolphin DH (1987) 2-Deoxy-2-Fluoroglucosides—a novel class of mechanism-based glucosidase inhibitors. *J Am Chem Soc* 109:7530–7531.
8. Zechel DL, Withers SG (2000) Glycosidase mechanisms: Anatomy of a finely tuned catalyst. *Accounts Chem Res* 33:11–18.
9. McCarter JD, Adam MJ, Withers SG (1992) Synthesis of 2-Deoxy-2-[F-18]-Fluoro-Beta-Mannosyl [F-18] fluoride as a potential imaging probe for glycosidases. *J Labelled Compd* 31:1005–1009.
10. Wong AW, Adam MJ, Withers SG (2001) Synthesis of 2, 6-dideoxy-2-fluoro-6-[F-18]-fluoro-beta-D-glucopyranosyl fluoride (2, 6FGF) as a potential imaging probe for glucocerebrosidase. *J Labelled Compd* 44:385–394.
11. Sharma SK, Corrales G, Penades S (1995) Single-step stereoselective synthesis of unprotected 2, 4-Dinitrophenyl glycosides. *Tetrahedron Lett* 36:5627–5630.
12. Berven LA, Dolphin D, Withers SG (1990) The base-catalyzed anomerization of dinitrophenyl glycosides—evidence for a novel reaction-mechanism. *Can J Chem* 68:1859–1866.
13. Koeners HJ, Dekok AJ, Romers C, Vanboom JH (1980) The use of the 2, 4-Dinitrophenyl group in sugar chemistry reexamined. *Recl Trav Chim Pay-B* 99:355–362.
14. Namchuk MN, Withers SG (1995) Mechanism of Agrobacterium beta-glucosidase: Kinetic analysis of the role of noncovalent enzyme/substrate interactions. *Biochemistry* 34:16194–16202.
15. Wang Q, Trimbur D, Graham R, Warren RAJ, Withers SG (1995) Identification of the acid/base catalyst in Agrobacterium-faecalis beta-glucosidase by kinetic-analysis of mutants. *Biochemistry* 34:14554–14562.
16. Wang QP, Graham RW, Trimbur D, Warren RAJ, Withers SG (1994) Changing enzymatic-reaction mechanisms by mutagenesis—conversion of a retaining glucosidase to an inverting enzyme. *J Am Chem Soc* 116:11594–11595.
17. Trimbur DE, Warren RAJ, Withers SG (1992) Region-directed mutagenesis of residues surrounding the active-site nucleophile in beta-glucosidase from Agrobacterium-faecalis. *J Biol Chem* 267:10248–10251.
18. Street IP, Kempton JB, Withers SG (1992) Inactivation of a beta-glucosidase through the accumulation of a stable 2-Deoxy-2-Fluoro-Alpha-D-Glucopyranosyl enzyme intermediate—a detailed investigation. *Biochemistry* 31:9970–9978.
19. Zhu XX, Sheth KA, Li SH, Chang HH, Fan JQ (2005) Rational design and synthesis of highly potent beta-glucocerebrosidase inhibitors. *Angew Chem International Edition* 44:7450–7453.
20. Choy FYM (1986) Purification of human placental glucocerebrosidase using a 2-step high-performance hydrophobic and gel-permeation column chromatography method. *Anal Biochem* 156:515–520.
21. Dvir H, et al. (2003) X-ray structure of human acid-beta-glucosidase, the defective enzyme in Gaucher Disease. *Embo Rep* 4:704–709.
22. Xu Y, et al. (1996) Turnover and distribution of intravenously administered mannose-terminated human acid beta-glucosidase in murine and human tissues. *Pediatr Res* 39:313–322.
23. Bijsterbosch MK, et al. (1996) Quantitative analysis of the targeting of mannose-terminal glucocerebrosidase. Predominant uptake by liver endothelial cells. *Eur J Biochem* 237:344–349.
24. Friedman BA, et al. (1999) A comparison of the pharmacological properties of carbohydrate remodeled recombinant and placental-derived beta-glucocerebrosidase: implications for clinical efficacy in treatment of Gaucher Disease. *Blood* 93:2807–2816.
25. Kacher Y, et al. (2008) Acid beta-glucosidase: insights from structural analysis and relevance to Gaucher Disease therapy. *Biol Chem* 389:1361–1369.
26. Trejtnar F, Laznicek M (2002) Analysis of renal handling of radiopharmaceuticals. *Q J Nucl Med* 46:181–194.
27. McCarter JD, Adam MJ, Hartman NG, Withers SG (1994) In-Vivo inhibition of beta-glucosidase and beta-mannosidase activity in rats by 2-Deoxy-2-Fluoro-Beta-Glycosyl fluorides and recovery of activity in-Vivo and in-Vitro. *Biochem J* 301:343–348.
28. Du H, et al. (2005) The role of mannosylated enzyme and the mannose receptor in enzyme replacement therapy. *Am J Hum Genet* 77:1061–1074.
29. Stahl P, Schlesinger PH, Sigardson E, Rodman JS, Lee YC (1980) Receptor-mediated pinocytosis of mannose glycoconjugates by macrophages—characterization and evidence for receptor recycling. *Cell* 19:207–215.
30. Aviezer D, et al. (2009) Novel enzyme replacement therapy for Gaucher Disease: ongoing phase III clinical trial with recombinant human glucocerebrosidase expressed in plant cells. *Mol Genet Metab* 96:S13–S14.
31. Shaaltiel Y, et al. (2007) Production of glucocerebrosidase with terminal mannose glycans for enzyme replacement therapy of Gaucher's Disease using a plant cell system. *Plant Biotechnol J* 5:579–590.
32. Sinclair GB, Colobong KE, Choy FYM, Clarke LA (2007) Generation of a conditional knockout of murine glucocerebrosidase: utility for the study of Gaucher disease. *Mol Genet Metab* 90:148–156.